

50-Gb/s PDM-DMT-SSB Transmission over 40km SSF using a Single Photodetector in C-band

Jiahao Huo^{1,2}, Xian Zhou^{1,2*}, Kangping Zhong², Tao Gui³, Yiguang Wang², Liang Wang⁴, Jinhui Yuan², Hongyu Zhang⁵, Keping Long¹, Changyuan Yu², Alan Pak Tao Lau³, and Chao Lu²

¹University of Science & Technology Beijing (USTB), No.30 Xue Yuan Road, Haidian, Beijing, 100083, China

²Department of Electronic and Information Engineering, The Hong Kong Polytechnic University, Hung Hom, Kowloon, Hong Kong

³Department of Electrical Engineering, The Hong Kong Polytechnic University, Hung Hom, Kowloon, Hong Kong

⁴Department of Electronic Engineering, The Chinese University of Hong Kong, Shatin, N.T., Hong Kong

⁵Fixed Network Research and Development Department, Huawei Technologies Co Ltd, Sheng Zhen, China

E-mail: zhouxian219@gmail.com

Abstract: We experimentally demonstrated transmission of 50-Gb/s PDM-DMT-SSB signal over 40km SSF in C-band using a single photodetector. The DMT signal in another polarization is placed at the guard band of the SSB-OFDM signal.

OCIS codes: (060.2330) Fiber Optics communications; (060.4080) Modulation; (060.4230) Multiplexing;

1. Introduction

High spectral efficiency (SE) transmission becomes more important in satisfying the increasing demand of the bandwidth-limited links for data center and other short reach applications [1-2]. In terms of cost, footprint and power consumption, intensity modulation and direct detection (IM/DD) is more promising than coherent detection for short reach applications. For reaching high SE in IM/DD, a number of advanced modulation formats such as pulse amplitude modulation (PAM) [3-4], carrier-less amplitude and phase modulation (CAP) [5], and discrete multi-tone (DMT) [6-7], have been widely employed and demonstrated. However, the frequency-selective power fading induced by chromatic dispersion (CD) is one of major impairments for IM/DD systems. For DMT systems, bit-loading technique can optimize bandwidth utilization, but power fading still reduces available bandwidth and capacity. Another way to combat CD induced power fading is single-sideband modulation (SSB). However, the typical SSB systems require an extra guard band to avoid the nonlinear subcarrier-to-subcarrier beating interference (SSBI). For improving SE of SSB systems, there are several methods added to compensate SSBI without the use of guard band, such as nonlinear equalization (NLE) [8], iterative equalization [9], etc. But these algorithms will significantly raise the system computational complexity.

In this paper, we propose a polarization-division multiplexing (PDM) DMT-SSB scheme to increase SE and achieve more robustness against CD than IM/DD systems. Here, SSB-OFDM and DMT signals are respectively modulated on two orthogonal states of polarization, and the DMT signal is placed at the guard band of SSB-OFDM signal. In the receiver, only one single photodetector is used to detect the PDM-DMT-SSB signal directly. Based on the proposed PDM-DMT-SSB scheme, 50-Gb/s transmission over 40km SSF in C-band with a bit error rate of 3.8×10^{-3} is successfully demonstrated at receiver sensitivity of -7dBm without optical amplifier and optical CD compensator. To the best of the authors' knowledge, this is the first experimental demonstration of using a single photodetector to receive dual-polarization signals, and one polarization efficiently uses the guard band of the SSB signal.

2. Principle of PDM-DMT-SSB System

In the transmitter, the SSB-OFDM signal on x polarization (x-pol.) is modulated by using I/Q modulator with a guard band equals in width to the OFDM bandwidth, and the DMT signal is employed with intensity modulation on y polarization (y-pol.). The optical spectra of the modulated SSB-OFDM signal and DMT signal are shown in Fig. 1 (a) and (b) respectively.

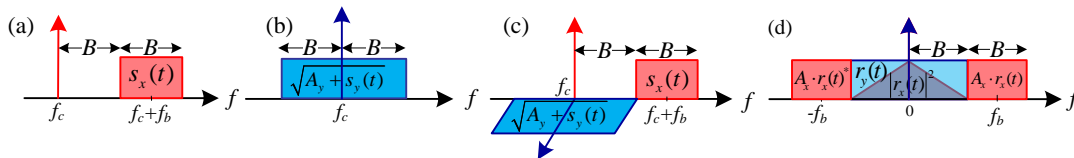


Fig.1. Optical spectra schematic diagrams of (a) SSB-OFDM signal, (b) DMT signal, (c) PDM-DMT-SSB signal, and (d) the electric spectrum of received PDM-DMT-SSB signal after direct detection.

After polarization beam combiner (PBC), the transmitted PDM-DMT-SSB signal (see Fig. 1(c)) can be expressed as

$$E_T(t) = \begin{bmatrix} E_x(t) \\ E_y(t) \end{bmatrix} = \begin{bmatrix} A_x + s_x(t)e^{j2\pi f_b t} \\ \sqrt{A_y + s_y(t)} \end{bmatrix} \quad (1)$$

where $A_{x(y)}$ denotes the DC bias, $s_x(t)e^{j2\pi f_b t}$ is the SSB-OFDM signal centered at frequency f_b , and $s_y(t)$ is the DMT signal.

For short reach links of a few tens of kilometers, the polarization crosstalk effect can be ignored. In this case, two orthogonal polarizations can be seen as two independent channels. In the receiver, the photodetector can be modeled as the square law detector, and the obtained photocurrent in x and y polarizations can be expressed as

$$d_x(t) = |E_x(t) \otimes h(t)|^2 = |A_x|^2 + A_x r_x(t) + A_x r_x^*(t) + |r_x(t)|^2 \quad (2)$$

$$d_y(t) = |E_y(t) \otimes h(t)|^2 \approx A_y + r_y(t) \quad (3)$$

where $r_x(t) = s_x(t)e^{j2\pi f_b t} \otimes h(t)$ and $r_y(t) = s_y(t) \otimes ((h(t) + h^*(t))/2)$. The electrical spectra of the detected SSB-OFDM (red) and DMT signals (blue) can be seen in Fig.1 (d). According to Eq. (2) and Eq. (3), the photocurrent of the whole PDM-DMT-SSB signal can be represented as

$$d(t) = d_x(t) + d_y(t) \approx \underbrace{|A_x|^2 + A_y + |r_x(t)|^2 + r_y(t)}_{\text{Low Frequency}} + \underbrace{A_x r_x(t) + A_x r_x^*(t)}_{\text{High Frequency}} \quad (4)$$

In Eq. (4), the third term is the SSB signal induced 2nd-order nonlinear SSBI, which overlaps with DMT signal after direct detection. But, it can be easily estimated and removed by using the received SSB signal in the high frequency components, namely the last two terms of Eq. (4). After SSBI elimination, the separated SSB-OFDM and DMT signals can be independently recovered by employing their traditional DSP algorithms.

3. Experimental setup and results

Fig. 2 illustrates the experimental setup of the proposed PDM-DMT-SSB scheme. In the transmitter, a 2^{16} pseudo-random binary sequence (PRBS) is mapped into 16QAM for SSB-OFDM and mapped into MQAM for DMT based on bit loading technique to optimize the link capacity under the limited bandwidth (Here, the 3-dB bandwidth of IM modulator is 6GHz). After mapping and serial to parallel (S/P) conversion, a 128-point IFFT is used to transfer the signal from frequency domain to time domain. A cyclic prefix (CP) of 6 samples is added to counter fiber dispersion-induced inter-symbol interference (ISI). The SSB-OFDM bandwidth is 14GHz with 7GHz guard band. The DMT signal bandwidth is designed to be 7GHz and placed at guard band of the SSB-OFDM signal. To satisfy the Hermitian symmetry property of the DMT, 59 subcarriers in positive frequency are loaded with the encoded data, 59 symmetric subcarriers in negative frequency are loaded with their conjugate information. The rest of subcarriers are null for dc and oversampling. A 1549.89nm center wavelength ECL with a polarization beam splitter (PBS) is used to generate the two orthogonal polarizations light. The SSB-OFDM and DMT signals are modulated to the two orthogonal polarizations respectively. A variable optical attenuator (VOA) is placed after I/Q modulator to adjust the SSB signal power. After PBC, the PDM-DMT-SSB signal is launched into 40km of SSMF transmission link. In the front end of the receiver, a VOA is placed after SSMF to adjust the received optical power (ROP). Then, the optical signal is detected by a PIN+TIA receiver, and sampled by a real-time scope for offline processing.

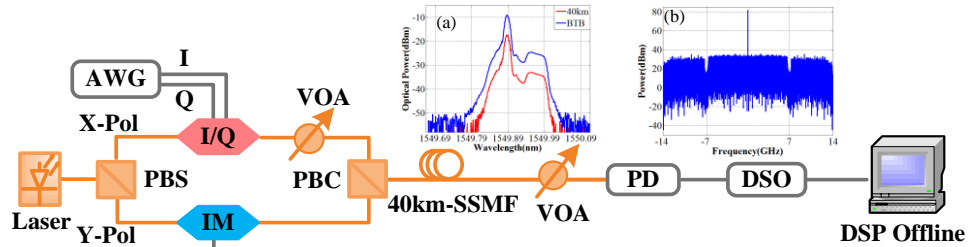


Fig.2. Experimental setup of PDM-DMT-SSB system and its (a) optical spectrum (b) electrical spectrum AWG: arbitrary waveform generator, I/Q: IQ modulator, IM: intensity modulator, DSO: digital sampling oscilloscope, DSP: digital signal processing.

The optical spectra of 50-Gb/s PDM-DMT-SSB signal for back to back (BTB) and after 40km SSMF transmission are shown in Fig. 2(a), where the sideband suppression ratio of the SSB-OFDM signal is more than 10dB. Fig. 2(b) shows the electrical spectrum of the PDM-DMT-SSB signal after a single photodetector direct detection. The illustration of SSBI elimination process can be seen as Fig. 3. Here, the filtered SSBI components between -7GHz to 7GHz are shown in Fig.3 (a). For observing clearly, there is no DMT signal. Fig.3 (b) shows the estimated SSBI impairment based on the received SSB-OFDM signal in high frequency. It can be seen from Fig.3 (c), the spectrum within [-7GHz, 7GHz] becomes flat after SSBI elimination. In order to further investigate the SSBI elimination performance, we constrain the DMT power to be -9dBm and change the SSB-OFDM power to measure BER performances of SSB signal and DMT signal with and without SSBI elimination respectively. It can be seen from Fig.4 (a), based on effective SSBI elimination, the BER performance of DMT can be kept about 5×10^{-4} during the SSB-OFDM power increased from -21 to -14dBm. After the SSB-OFDM power large over -13dBm, the BER of DMT starts to increase, which is caused by power saturation problem of photodetector. The BER as a function of ROP for BTB and 40km transmissions are both shown in Fig. 4(b). For a BER of 3.8×10^{-3} , the required ROPs of BTB and 40km are -8dBm and -7dBm respectively. The transmission penalty at a BER of 3.8×10^{-3} is therefore 1dB. However, there is a BER floor of 3×10^{-3} after 40 km SSMF transmission.

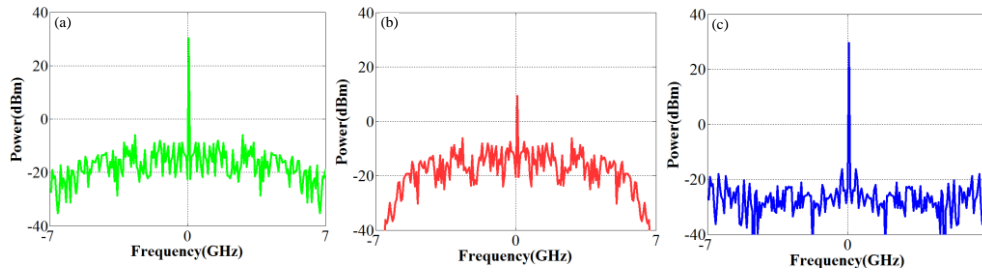


Fig.3. Illustration of SSBI elimination process, the electrical spectra of (a) the filtered SSBI without DMT signal (b) the estimated SSBI (c) after SSBI elimination by the use of estimated SSBI

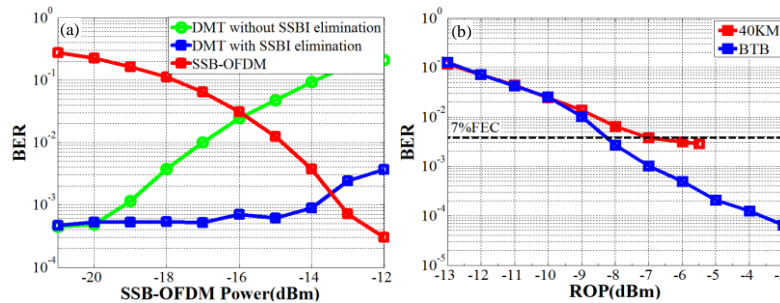


Fig.4. The experimental results of 50-Gb/s PDM-DMT-SSB system (a) BER vs. SSB-OFDM power for DMT power kept at -9dBm (b) BER vs. ROP for SSB-OFDM power and DMT power with a fixed ratio in BTB and 40km case

4. Conclusion

In this paper, we experimentally demonstrated 50-Gb/s PDM-DMT-SSB transmission using a single photodetector. This work simultaneously employs the PDM scheme and utilizes the guard band to improve the SE. The proposed PDM-DMT-SSB system is a promising cost-efficient solution for future short reach optical transmission system with high spectral efficiency.

Acknowledgement

This work is support by the 61671053 61401020 61435006 from National Natural Science Foundation of China, XJ2013026 from Hong Kong Scholars Program, and PolyU 152109/14E 152248/15E from Research Grant Council of Hong Kong SAR.

References

- [1] D. Che *et al.*, JLT, **33**(3), pp.678-684, (2015).
- [2] Chagnon M. *et al.*, OFC, paper, Th5B.2 (2015).
- [3] Zhou X. *et al.*, ACP, AM3E.3, (2015).
- [4] Rios-Müller R. *et al.*, OFC, paper, Th1G.4 (2016).
- [5] Zhong K P. *et al.*, Opt. Express **32**(2), pp. 1176-1189, (2015).
- [6] Zhou X. *et al.*, PJ, **7**(6), pp.1-12, (2015).
- [7] Lee J. *et al.*, OFC, paper, Th1G.1 (2016).
- [8] Zhang L. *et al.*, OFC, paper, Th4A2, (2015).
- [9] Li Z. *et al.*, Opt. Express **23**(18), pp. 23694-23709, (2015).